Title	DOA estimation and tracking of ULAs with mutual coupling
Author(s)	Liao, B; Zhang, ZG; Chan, SC
Citation	IEEE Transactions on Aerospace and Electronic Systems, 2012, v. 48 n. 1, p. 891-905
Issued Date	2012
URL	http://hdl.handle.net/10722/137289
Rights	©2012 IEEE. Personal use of this material is permitted. However, permission to reprint/republish this material for advertising or promotional purposes or for creating new collective works for resale or redistribution to servers or lists, or to reuse any copyrighted component of this work in other works must be obtained from the IEEE.

DOA Estimation and Tracking of ULAs with Mutual Coupling

BIN LIAO, Student Member, IEEE
ZHI-GUO ZHANG, Member, IEEE
SHING-CHOW CHAN, Member, IEEE
The University of Hong Kong

A class of subspace-based methods for direction-of-arrival (DOA) estimation and tracking in the case of uniform linear arrays (ULAs) with mutual coupling is proposed. By treating the angularly-independent mutual coupling as angularly-dependent complex array gains, the middle subarray is found to have the same complex array gains. Using this property, a new way for parameterizing the steering vector is proposed and the corresponding method for joint estimation of DOAs and mutual coupling matrix (MCM) using the whole array data is derived based on subspace principle. Simulation results show that the proposed algorithm has a better performance than the conventional subarray-based method especially for weak signals. Furthermore, to achieve low computational complexity for online and time-varying DOA estimation, three subspace tracking algorithms with different arithmetic complexities and tracking abilities are developed. More precisely, by introducing a better estimate of the subspace to the conventional tracking algorithms, two modified methods, namely modified projection approximate subspace tracking (PAST) (MPAST) and modified orthonormal PAST (MOPAST), are developed for slowly changing subspace, whereas a Kalman filter with a variable number of measurements (KFVM) method for rapidly changing subspace is introduced. Simulation results demonstrate that these algorithms offer high flexibility and effectiveness for tracking DOAs in the presence of mutual coupling.

Manuscript received October 11, 2010; revised January 6, 2011; ready for publication March 18, 2011.

IEEE Log No. T-AES/48/1/943654.

Refereeing of this contribution was handled by U. Nickel.

Authors' address: Department of Electrical and Electronic Engineering, The University of Hong Kong, Pokfulam Road, Hong Kong, E-mail: (scchan@eee.hku.hk).

I. INTRODUCTION

Mutual coupling, which is caused by interactions among array elements, may seriously degrade the performance of high-resolution direction finding techniques such as MUSIC [1], ESPRIT [2], and position determination approaches [3]. In ideal situations, the steering vector is assumed to be exactly known which depends on the array geometry and the signal location. However, such an assumption is often far from reality, as the steering vector in real systems may be distorted by impairments such as mutual coupling, array gain/phase uncertainties [4], and sensor position perturbation [5]. Since the presence of mutual coupling would lead to considerable deteriorations in direction finding of conventional high-resolution direction-of-arrival (DOA) estimation algorithms, mutual coupling calibration has received extensive attention over the last decades [6–21].

The method of moments (MoM) [6] has been widely used to evaluate mutual coupling and compensation [7, 8]. However, the computation requires a priori knowledge of the incoming signals such as DOAs. Another kind of method for mutual coupling calibration makes use of exactly known source locations, namely, calibration sources [9, 10]. By applying calibration sources, the maximum-likelihood (ML)-based method proposed in [9] can be used to compensate for mutual coupling, array gain/phase uncertainties, as well as sensor position errors. Also, the calibration matrix can be estimated using a set of calibration sources with known locations in [10]. Unfortunately, calibration sources may be difficult or even impossible to obtain in real systems. Alternatively, a kind of array calibration method, the so-called auto-calibration or online-calibration, is more preferable, since it does not require calibration sources [11, 12]. The classical mutual coupling auto-calibration method proposed by Friedlander and Weiss [11] and a more recent one proposed by Sellone and Serra [12] are able to estimate DOAs and mutual coupling coefficients using an iterative procedure. However, since a large number of unknown parameters are involved in these two methods, their high computational complexities may be prohibitive for real-time applications and the convergence may not be guaranteed [13, 14].

In order to overcome the drawbacks of mutual coupling auto-calibration methods described above, recent attention has been focusing on simplified methods with lower complexities. In [15] and [16], mutual coupling calibration methods for specific geometry arrays, such as uniform linear array (ULA) and uniform circular array (UCA), were presented. These methods are based on the fact that the mutual coupling coefficient between two sensor elements is inversely related to their distance and can be approximated as zero when they are separated by

few wavelengths. Consequently, the number of unknown parameters is significantly reduced. Another class of methods using instrumental sensors for array calibration has also been developed [17–19]. It exploits the fact that only part of the new array has mutual coupling or other errors after adding instrumental sensors into the original array. For example, the mutual coupling calibration method using instrumental sensors in [18] requires only a one-dimensional search. For the case of three instrumental sensors, the sources are required to be time-disjoint, i.e., only one source impinges on the array at each time interval, whereas more instrumental sensors are required for time-joint sources. More recently, another mutual coupling calibration algorithm with instrumental sensors was developed in [19]. The middle subarray is first utilized for DOA estimation using the MUSIC algorithm. Further refinement of DOA estimates can then be performed using the whole array.

In this paper, we present a new method for DOA estimation for ULAs in the presence of mutual coupling. The symmetric Toeplitz structure of mutual coupling matrix (MCM) of a ULA as in [19] is employed. However, we found that the DOAs of incoming signals and mutual coupling coefficients can be estimated jointly by taking advantage of the special structure of MCM using a new parameterization of the steering vector and the subspace principle [20]. Simulation results show that the proposed algorithm gives a better performance, especially for signals with low signal-to-noise ratio (SNR), than the method in [19], since the whole array rather than a subarray in [19] can be used to estimate DOAs and compensate for the mutual coupling effect.

Most of the array calibration algorithms discussed so far assume that DOAs are time invariant. However, the DOAs may be time varying in real systems [27–31]. When the subspace is computed from the eigenvalue decomposition (EVD) of the covariance matrix of the entire observations, the performance of calibration algorithms will be deteriorated significantly. Moreover, computing the EVD directly online usually involves high arithmetic complexity. To reduce the computational complexity of the subspace using EVD for online and time-varying DOA estimation, extended subspace tracking algorithms with better performance are incorporated into the proposed joint estimation procedure. A number of algorithms have been proposed for tracking DOAs [27–29] and subspace [30–33], but the effect of mutual coupling has not been considered in these methods. A classical algorithm is the projection approximate subspace tracking (PAST) method proposed by B. Yang [30]. Based on the assumption that the subspace varies slowly, the PAST algorithm employs the so-called "projection approximation" to compute the signal subspace using the recursive least squares (RLS) algorithm. When an orthonormal basis of the subspace is required, an additional step of reorthonormalization has to be performed. In [33], an extension of the PAST algorithm called the orthonormal PAST (OPAST) algorithm was proposed to produce an orthonormal subspace directly with reduced complexity. Since the above RLS-based PAST algorithms require the subspace to be slow varying and the estimate is solely based on the observations, its performance will be degraded significantly when the subspace changes rapidly. Moreover, when mutual coupling exists, conventional DOA estimation algorithms cannot be directly applied.

In this paper, three subspace tracking algorithms with different arithmetic complexities and tracking abilities are studied for estimating time-varying DOAs in the presence of mutual coupling. The first two are called the modified PAST (MPAST) and modified OPAST (MOPAST) algorithms for slowly changing subspace, and the last one is an adaptive Kalman filter-based algorithm for fast changing subspace. In the MPAST and MOPAST algorithms, we find that a better tracking performance can be obtained by repeating the respective PAST and OPAST iteration one or more times, since the "projection approximation" will be further improved with the subspace estimates. In the adaptive Kalman filter-based algorithm, the signal subspace is regarded as the system state and an adaptive Kalman filter with variable number of measurements (KFVM) [35, 36] is employed for tracking the fast-varying subspace. Hence, the fast-varying DOAs can be estimated using the framework previously developed in the paper. The KFVM differs from the conventional Kalman filter in that the number of measurements used is chosen adaptively, which leads to a better performance of DOA tracking. Simulation results show that these two algorithms provide effective tradeoff between performance and the arithmetic complexities for tracking DOAs in the presence of mutual coupling in different testing conditions.

The rest of the paper is organized as follows. The problem formulation is first introduced in Section II. The proposed method for DOA estimation in the presence of mutual coupling, using a new parameterization based on the symmetric Toeplitz structure of MCM of ULA in [19] and the subspace principle, is given in Section III. Next, we consider situations where DOAs are time varying. Three subspace tracking approaches, namely the MPAST, MOPAST, and KFVM, are presented to deal with these situations in Section IV. Simulations are conducted to demonstrate the effectiveness of the proposed methods in Section V, and finally, Section VI concludes the paper.

II. PROBLEM FORMULATION

Consider a ULA with M sensors impinged by N narrowband signals $s_n(t)$, $n = 1,2,\ldots,N$, where t is the time variable. The N sources are assumed to be from far field with unknown directions θ_n, $n = 1,2,\ldots,N$. Assuming identical sensors and no other errors such as location uncertainties, the ideal steering vector at an angle θ can be obtained from the array geometry as

$$\mathbf{a}(\theta) = [1, \beta(\theta), \ldots, \beta(\theta)^{M-1}]^{\mathrm{T}} \tag{1}$$

where $\beta(\theta) = \exp(-j2\pi\lambda^{-1}d\sin\theta)$, d is the inter-sensor spacing, λ is the signal carrier wavelength, $j = \sqrt{-1}$ and $(\cdot)^{\mathrm{T}}$ denotes matrix transposition. The vector of observed array output can be written as

$$\mathbf{x}(t) = \mathbf{A}\mathbf{s}(t) + \mathbf{n}(t) \tag{2}$$

where

$$\mathbf{A} = [\mathbf{a}(\theta_1), \mathbf{a}(\theta_2), \ldots, \mathbf{a}(\theta_N)]$$

$$\mathbf{s}(t) = [s_1(t), s_2(t), \ldots, s_N(t)]^{\mathrm{T}}$$

are the ideal steering matrix and vector of signal waveforms, respectively, and $\mathbf{n}(t)$ is an independent and identically distributed (IID) additive white Gaussian noise (AWGN) vector with zero mean and covariance matrix $\sigma^2\mathbf{I}$, where $\mathbf{I}$ is an identity matrix.

In practice, interactions between the sensors will result in mutual coupling, which distorts the ideal steering vector significantly. In this situation, the true steering vector should be modified as

$$\mathbf{a}_m(\theta) = \mathbf{C}\mathbf{a}(\theta) \tag{3}$$

where $\mathbf{C}$ is the MCM, and it is a symmetric Toeplitz matrix having the form [19]

$$\mathbf{C} = \begin{bmatrix} 1 & c_1 & \cdots & c_{P-1} & \cdots & c_{M-1} \\ c_1 & 1 & c_1 & \cdots & \ddots & \vdots \\ \vdots & c_1 & 1 & c_1 & \cdots & c_{P-1} \\ c_{P-1} & \cdots & \ddots & \ddots & \ddots & \vdots \\ \vdots & \ddots & \cdots & c_1 & 1 & c_1 \\ c_{M-1} & \cdots & c_{P-1} & \cdots & c_1 & 1 \end{bmatrix}_{M\times M} \tag{4}$$

where $c_i = \rho_i e^{j\phi_i}$ $(i = 1,2,\ldots,M-1)$ is the mutual coupling coefficient, ρ_i and ϕ_i denote, respectively, the amplitude and phase of the mutual coupling coefficient c_i. With the MCM structure in (4), the classical iterative approach in [11] can be employed for DOA estimation. However, the complexity may be high for some real-time applications. On the other hand, it is known that the mutual coupling coefficient between two sensors is inversely related to their distance, and thus it is negligible for two sensors which are separated by several sensors away. More precisely, when the distance between two sensors is more than P inter-sensor spacings, the mutual coupling coefficient can be approximated to be zero, i.e.,

$$c_i = 0, \qquad P \le i \le M-1. \tag{5}$$

As a result, the resultant MCM can be simplified to a banded symmetric Toeplitz matrix as follows [19]

$$\mathbf{C} = \begin{bmatrix} 1 & c_1 & \cdots & c_{P-1} & & & & \\ c_1 & 1 & c_1 & \cdots & c_{P-1} & & {}^{\circ}0 & \\ \vdots & \ddots & \ddots & \ddots & \vdots & \ddots & & \\ c_{P-1} & \cdots & c_1 & 1 & c_1 & \cdots & c_{P-1} & \\ & \ddots & \vdots & \ddots & \ddots & \ddots & & \ddots \\ & & c_{P-1} & \cdots & c_1 & 1 & c_1 & \cdots & c_{P-1} \\ & & & \ddots & \vdots & \ddots & \ddots & \ddots & \vdots \\ & \mathbf{0} & & & c_{P-1} & \cdots & c_1 & 1 & c_1 \\ & & & & & c_{P-1} & \cdots & c_1 & 1 \end{bmatrix}_{M\times M}. \tag{6}$$

Replacing $\mathbf{a}(\theta)$ in (2) with $\mathbf{a}_m(\theta)$, the array output can then be represented by the following model

$$\mathbf{x}(t) = \mathbf{C}\mathbf{A}\mathbf{s}(t) + \mathbf{n}(t). \tag{7}$$

We next give a brief introduction to various subspace quantities before we apply them to the mutual coupling compensation. The array covariance matrix of $\mathbf{x}(t)$ in (7) can be written as

$$\mathbf{R}_X = E[\mathbf{x}(t)\mathbf{x}^{\mathrm{H}}(t)] = \mathbf{C}\mathbf{A}\mathbf{R}_S\mathbf{A}^{\mathrm{H}}\mathbf{C}^{\mathrm{H}} + \sigma^2\mathbf{I} \tag{8}$$

where $(\cdot)^{\mathrm{H}}$ denotes the Hermitian transpose operation, and $\mathbf{R}_S = E[\mathbf{s}(t)\mathbf{s}^{\mathrm{H}}(t)]$ is the signal covariance matrix. Assuming the N signals are uncorrelated, then the rank of $\mathbf{R}_S$ is N. Consequently, the EVD of $\mathbf{R}_X$ can be described as

$$\mathbf{R}_X = \mathbf{U}_S\Sigma_S\mathbf{U}_S^{\mathrm{H}} + \mathbf{U}_V\Sigma_V\mathbf{U}_V^{\mathrm{H}} \tag{9}$$

where $\mathbf{U}_S \in \mathbb{C}^{M\times N}$ and $\mathbf{U}_V \in \mathbb{C}^{M\times(M-N)}$ are the signal subspace and noise subspace, respectively; $\Sigma_S \in \mathbb{R}^{M\times M}$ and $\Sigma_V \in \mathbb{R}^{(M-N)\times(M-N)}$ are diagonal matrices related to the signal and noise power, respectively. In real systems, the covariance matrix $\mathbf{R}_X$ can be estimated from a finite set of sample snapshots as

$$\hat{\mathbf{R}}_X = \frac{1}{T}\sum_{t=1}^{T}\mathbf{x}(t)\mathbf{x}^{\mathrm{H}}(t) \tag{10}$$

where T is the total number of snapshots. Then the estimated signal subspace $\hat{\mathbf{U}}_S$ and the estimated noise subspace $\hat{\mathbf{U}}_V$ can be obtained from the corresponding EVD of $\hat{\mathbf{R}}_X$. For more details of the subspace method, interested readers are referred to [1], [2].

III. DOA ESTIMATION AND MUTUAL COUPLING COMPENSATION

In this section a new parameterization of the steering vector using the banded symmetric Toeplitz structure of the MCM of ULAs in (6) is introduced. It utilizes the whole array and the subspace principle to estimate the DOAs and mutual coupling coefficients. According to the MCM and signal models above, the steering vector of the array can be rewritten as

$$\mathbf{a}_m(\theta) = \left[1 + \sum_{i=1}^{P-1} c_i(\beta(\theta)^i + \beta(\theta)^{-i})\right] \Gamma(\theta)\mathbf{a}(\theta) \tag{11}$$

where

$$\Gamma(\theta) = \text{diag}[\mu_1,\ldots,\mu_{P-1},1,\ldots,1,\alpha_1,\ldots,\alpha_{P-1}] \tag{12}$$

is a diagonal matrix containing $M-2P+2$ ones between the entry μ_{P-1} and α_1, and

$$\mu_k = \frac{\beta(\theta)^{P-1} + \sum_{i=1}^{k-1} c_i\beta(\theta)^{P-1-i} + \sum_{i=1}^{P-1} c_i\beta(\theta)^{P-1+i}}{\beta(\theta)^{P-1} + \sum_{i=1}^{P-1} c_i\beta(\theta)^{P-1-i} + \sum_{i=1}^{P-1} c_i\beta(\theta)^{P-1+i}} \tag{13a}$$

and

$$\alpha_k = \frac{\beta(\theta)^{P-1} + \sum_{i=1}^{P-1} c_i\beta(\theta)^{P-1-i} + \sum_{i=1}^{P-1-k} c_i\beta(\theta)^{P-1+i}}{\beta(\theta)^{P-1} + \sum_{i=1}^{P-1} c_i\beta(\theta)^{P-1-i} + \sum_{i=1}^{P-1} c_i\beta(\theta)^{P-1+i}} \tag{13b}$$

for $k = 1,2,\ldots,P-1$. For notational simplicity, we define $\sum_{i=1}^{0} c_i\beta(\theta)^{P-1\pm i} = 0$ in (13). (The detailed derivation of (11)–(13) is available at http://www.eee.hku.hk/∼liaobin/Mutual_Coupling.pdf.) From (12) it can be noted that angularly independent mutual coupling can be viewed as angularly dependent complex array gains. However, it is in general difficult to calibrate the angularly dependent array gains to account for the mutual coupling. Interestingly, there is a string of ones in the diagonal matrix $\Gamma(\theta)$, indicating that the middle subarray can be considered as an array with same (or say, without) array gains. We now show that it is possible to jointly estimate the DOAs and mutual coupling coefficients based on this property.

Since $\Gamma(\theta)$ is a diagonal matrix with $M-2P+2$ ones and $\mathbf{a}(\theta)$ is a column vector, (11) can be rewritten as the following parameterization for joint estimation of MCM and DOAs:

$$\mathbf{a}_m(\theta) = \left[1 + \sum_{i=1}^{P-1} c_i(\beta(\theta)^i + \beta(\theta)^{-i})\right] \mathbf{T}(\theta)\boldsymbol{\alpha} \tag{14}$$

where

$$\mathbf{T}(\theta) = \begin{bmatrix} 1 & & & & & \\ & \beta(\theta) & & & & \\ & & \ddots & & \mathbf{0} & \\ & & & \beta(\theta)^{P-1} & & \\ & & & \vdots & & \\ & & & \beta(\theta)^{M-P} & & \\ & & \mathbf{0} & & \ddots & \\ & & & & & \beta(\theta)^{M-1} \end{bmatrix}_{M\times(2P-1)} \tag{15}$$

is an $M \times (2P-1)$ matrix and

$$\boldsymbol{\alpha} = [\mu_1,\ldots,\mu_{P-1},1,\alpha_1,\ldots,\alpha_{P-1}]^{\text{T}} \tag{16}$$

is a $(2P-1)\times 1$ vector with the Pth entry equal to 1.

Next, we employ the subspace principle to determine the required parameters. As mentioned in Section II, the signal subspace $\mathbf{U}_S$ and the noise subspace $\mathbf{U}_N$ can be obtained from the EVD of covariance matrix $\mathbf{R}_X$ in (9). From the principle of subspace, the steering vector of the incoming signal is orthogonal to the noise subspace. Hence, we have the following equation for solving the mutual coupling coefficients and DOAs:

$$\mathbf{a}_m^{\text{H}}\mathbf{U}_V\mathbf{U}_V^{\text{H}}\mathbf{a}_m = 0. \tag{17}$$

Firstly, $1 + \sum_{i=1}^{P-1} c_i(\beta(\theta)^i + \beta(\theta)^{-i})$ is assumed to be non-zero; the case of zero is discussed later in this section. Then, substituting (14) into (17), one gets

$$\boldsymbol{\alpha}^{\text{H}}\mathbf{Q}(\theta)\boldsymbol{\alpha} = 0 \tag{18}$$

where

$$\mathbf{Q}(\theta) = \mathbf{T}^{\text{H}}(\theta)\mathbf{U}_V\mathbf{U}_V^{\text{H}}\mathbf{T}(\theta) \tag{19}$$

is a $(2P-1)\times(2P-1)$ matrix.

We now show that it is possible to estimate the DOAs based on the determinant or the smallest eigenvalue of $\mathbf{Q}(\theta)$. It can be found that the dimension of $\mathbf{U}_V^{\text{H}}\mathbf{T}(\theta)$ is $(M-N)\times(2P-1)$ and if it satisfies $2P-1 \le M-N$, i.e.,

$$N \le M-2P+1 \tag{20}$$

the matrix $\mathbf{U}_V^{\text{H}}\mathbf{T}(\theta)$, in general, is full column rank and $\mathbf{Q}(\theta)$ is full rank. However, when θ coincides with any one of the N desired DOAs, i.e., $\theta = \theta_n (n = 1,2,\ldots,N)$, the matrix $\mathbf{Q}(\theta)$ will be rank deficiency, and its determinant is equal to zero. Consequently, the determinant of $\mathbf{Q}(\theta)$ can be adopted for DOA estimation. In the finite snapshots case, DOAs of signals can be estimated from the following spatial spectrum

$$P_{\text{DET}}(\theta) = \{\det[\hat{\mathbf{Q}}(\theta)]\}^{-1} \tag{21}$$

where $\hat{\mathbf{Q}}(\theta) = \mathbf{T}^{\text{H}}(\theta)\hat{\mathbf{U}}_V\hat{\mathbf{U}}_V^{\text{H}}\mathbf{T}(\theta)$, $\det[\cdot]$ denotes determinant of a matrix and the nth estimated DOA

$\hat{\theta}_n$ is associated with the nth peak of the spectrum $P_{\mathrm{DET}}(\theta)$. On the other hand, since the smallest eigenvalue of $\mathbf{Q}(\theta)$ is also equal to zero when $\theta = \theta_n$ $(n = 1,2,\ldots,N)$, the DOAs can also be estimated from the following spatial spectrum

$$P_{\mathrm{EV}}(\theta) = \lambda_{\min}^{-1}[\hat{\mathbf{Q}}(\theta)] \tag{22}$$

where $\lambda_{\min}[\cdot]$ denotes the smallest eigenvalue of a matrix.

It is worth noting that (22) is a necessary condition for determining the DOAs, though mathematically it is very difficult to show that the rank deficiency of $\mathbf{Q}(\theta)$ is sufficient to indicate that the corresponding θ is one of the desired DOAs. It was found in our simulations that the peaks of the spectra (21) and (22) only occur when θ coincides with the DOAs. This determinant- and eigenvalue-based rank dropping criterion was also observed in related work and has been successfully applied to DOA estimation using partly calibrated antenna arrays [22–26]. We also notice that a ULA with mutual coupling can also be regarded as a partly calibrated array since the middle subarray sensors have the same complex array gains as shown in (12).

Actually, even if pseudopeaks of the spectra (21) and (22) are encountered, one can also identify these pseudopeaks by performing a rough estimation of the DOAs using MUSIC without considering the mutual coupling or using the conventional method in [19] using the middle subarray. By comparing the two results, such pseudopeaks can generally be identified.

We now proceed to estimate the mutual coupling coefficients based on the estimated DOAs. It can be seen that (17) is satisfied when $\boldsymbol{\alpha}$ is the eigenvector corresponding to the smallest eigenvalue of $\mathbf{Q}(\hat{\theta})$, which is denoted by $\mathbf{r}_{\min}$ here. Since the Pth entry of $\boldsymbol{\alpha}$ is equal to 1, $\boldsymbol{\alpha}$ can be estimated as

$$\hat{\boldsymbol{\alpha}} = \mathbf{r}_{\min} \qquad \text{with} \quad [\mathbf{r}_{\min}]_P = 1 \tag{23}$$

where $[\mathbf{r}_{\min}]_P$ denotes the Pth entry of vector $\mathbf{r}_{\min}$. From (13b), (16), and (23), it can be seen that the mutual coupling coefficients are embedded in $\boldsymbol{\alpha}$. We now proceed to estimate the mutual coupling coefficient vector $\mathbf{c}$

$$\mathbf{c} = [c_1, c_2, \ldots, c_{P-1}]^{\mathrm{T}}. \tag{24}$$

First of all, define

$$\mathbf{v} = [v_1, \ldots, v_k, \ldots, v_{P-1}]^{\mathrm{T}} \tag{25}$$

where $v_k = [\mathbf{r}_{\min}]_{k+P}$ denotes the kth element of $\mathbf{v}$ and is equal to the $(k+P)$th element of $\mathbf{r}_{\min}$. From (13b), (23), and (25), we know that, for any $k = 1,2,\ldots,P-1$, we have $\hat{\alpha}_k = v_k$, then

$$(1 - v_k)\sum_{i=1}^{P-1} c_i \beta(\hat{\theta})^{P-1-i} + \sum_{i=1}^{P-1-k} c_i \beta(\hat{\theta})^{P-1+i} - v_k \sum_{i=1}^{P-1} c_i \beta(\hat{\theta})^{P-1+i} = (v_k - 1)\beta(\hat{\theta})^{P-1}. \tag{26}$$

The equation above can also be written in vector form as

$$[(1 - v_k)\beta_1(\hat{\theta}) + \beta_{2,k}(\hat{\theta}) - v_k \beta_3(\hat{\theta})]^{\mathrm{T}}\mathbf{c} = (v_k - 1)\beta(\hat{\theta})^{P-1} \tag{27}$$

where

$$\beta_1(\hat{\theta}) = [\beta(\hat{\theta})^{P-2} \quad \beta(\hat{\theta})^{P-3} \cdots 1]^{\mathrm{T}}$$

$$\beta_{2,k}(\hat{\theta}) = [\beta(\hat{\theta})^{P} \quad \beta(\hat{\theta})^{P+1} \cdots \beta(\hat{\theta})^{2(P-1)-k} \quad 0_k]^{\mathrm{T}}$$

$$\beta_3(\hat{\theta}) = [\beta(\hat{\theta})^{P} \quad \beta(\hat{\theta})^{P+1} \cdots \beta(\hat{\theta})^{2(P-1)}]^{\mathrm{T}}$$

are $(P-1)\times 1$ vectors, and 0_k is the $1 \times k$ zero vector. It should be noted that when $2(P-1) - k < P$, i.e., $k > P-2$, $\beta_{2,k}(\hat{\theta}) = [0_{P-1}]^{\mathrm{T}}$, and when $2(P-1) - k = P$, i.e., $k = P-2$, $\beta_{2,k}(\hat{\theta}) = [\beta(\hat{\theta})^{P} \;\; 0_k]^{\mathrm{T}}$. Denote

$$\mathbf{f}_k = (1 - v_k)\beta_1(\hat{\theta}) + \beta_{2,k}(\hat{\theta}) - v_k \beta_3(\hat{\theta}) \tag{28}$$

$$g_k = (v_k - 1)\beta(\hat{\theta})^{P-1}. \tag{29}$$

Since $1 \le k \le P-1$, (27) can be extended to form

$$[\mathbf{f}_1 \cdots \mathbf{f}_{P-1}]^{\mathrm{T}}\mathbf{c} = [g_1 \cdots g_{P-1}]^{\mathrm{T}}. \tag{30}$$

Therefore, the mutual coupling coefficient vector $\mathbf{c}$ can be estimated by solving (30) with a general estimated DOA $\hat{\theta}$ as

$$\mathbf{c} = \mathbf{F}^{-1}\mathbf{G} \tag{31}$$

where $\mathbf{F} = [\mathbf{f}_1 \cdots \mathbf{f}_{P-1}]^{\mathrm{T}}$ is a $(P-1)\times(P-1)$ matrix, and $\mathbf{G} = [g_1 \cdots g_{P-1}]^{\mathrm{T}}$ is a $(P-1)\times 1$ vector.

In order to get a better performance, all of the estimated DOAs will be employed to calculate the mutual coupling coefficients. Therefore, we extend (30) with the N estimated DOAs as

$$\bar{\mathbf{F}}\mathbf{c} = \bar{\mathbf{G}} \tag{32}$$

where $\bar{\mathbf{F}} = [\mathbf{F}_1^{\mathrm{T}} \cdots \mathbf{F}_N^{\mathrm{T}}]^{\mathrm{T}}$, $\bar{\mathbf{G}} = [\mathbf{G}_1^{\mathrm{T}} \cdots \mathbf{G}_N^{\mathrm{T}}]^{\mathrm{T}}$, $\mathbf{F}_n$ and $\mathbf{G}_n$ represent $\mathbf{F}$ and $\mathbf{G}$ evaluated, respectively, at the nth estimated DOA $\hat{\theta}_n$. Solving the linear system in (32), one finally gets

$$\mathbf{c} = (\bar{\mathbf{F}}^{\mathrm{H}}\bar{\mathbf{F}})^{-1}\bar{\mathbf{F}}^{\mathrm{H}}\bar{\mathbf{G}}. \tag{33}$$

The estimation performance of the DOAs and mutual coupling coefficients above can be further improved by iterations. More precisely, once the estimate of $\mathbf{c}$ is obtained, the MUSIC algorithm with the estimated mutual coupling can be applied, and a more accurate estimate of DOAs can be obtained from the MUSIC spatial spectrum as

$$P_{\mathrm{MUSIC}}(\theta) = \|\hat{\mathbf{U}}_V^{\mathrm{H}}\hat{\mathbf{C}}\mathbf{a}(\theta)\|^{-2}. \tag{34}$$

Then, the mutual coupling coefficients $\mathbf{c}$ can be recomputed using the new estimate of DOAs from (34). This procedure can be repeated to further enhance the performance. Simulation results in the next section show that a satisfactory performance

TABLE I
The Joint DOA and Mutual Coupling Estimation Algorithm

Step 1)	Collect T snapshots and calculate the covariance matrix $\hat{\mathbf{R}}_X$ as (10).
Step 2)	Obtain the signal subspace $\hat{\mathbf{U}}_S$ and noise subspace $\hat{\mathbf{U}}_V$ from the EVD of $\hat{\mathbf{R}}_X$.
Step 3)	Use the subspace $\hat{\mathbf{U}}_V$ and (21) or (22) to estimate the N DOAs.
Step 4)	For each estimated $\hat{\theta}_n$, $(n = 1,\ldots,N)$, calculate $\mathbf{Q}(\hat{\theta}_n)$ using (19), and obtain the eigenvector $\mathbf{r}_{\min}$ from the EVD of $\mathbf{Q}(\hat{\theta}_n)$.
Step 5)	For each k, $(k = 1,\ldots,P-1)$, calculate $\mathbf{f}_k^{(n)}$ and $g_k^{(n)}$, using (28) and (29), respectively, and obtain $\mathbf{F}_n$ and $\mathbf{G}_n$ as $\mathbf{F}_n = [\mathbf{f}_1^{(n)}\cdots\mathbf{f}_{P-1}^{(n)}]^{\mathrm{T}}$ and $\mathbf{G}_n = [g_1^{(n)}\cdots g_{P-1}^{(n)}]^{\mathrm{T}}$, respectively.
Step 6)	Obtain $\bar{\mathbf{F}}$, $\bar{\mathbf{G}}$ as $\bar{\mathbf{F}} = [\mathbf{F}_1^{\mathrm{T}}\cdots\mathbf{F}_N^{\mathrm{T}}]^{\mathrm{T}}$ and $\bar{\mathbf{G}} = [\mathbf{G}_1^{\mathrm{T}}\cdots\mathbf{G}_N^{\mathrm{T}}]^{\mathrm{T}}$, respectively. Calculate the mutual coupling coefficient vector c and MCM using (33) and (36), respectively.
Step 7)	Improve the DOA estimation accuracy with the estimated MCM and (34).
Step 8)	Repeat Step 4 to Step 7 to further improve the performance of DOA and mutual coupling estimation.

can be obtained with an additional iteration. The proposed algorithm mentioned above is summarized in Table I.

It is worth noting that the above approach is derived based on the assumption that $1 + \sum_{i=1}^{P-1} \cdot c_i(\beta(\theta)^i + \beta(\theta)^{-i})$ is non-zero, whereas this function may be zero for those peculiar angles (blind angles) under some special mutual coupling coefficients c_i, $i = 1,\ldots,P-1$. As discussed in [19, Sect. IV], the middle subarray cannot receive any signals from those blind angles which satisfy the condition $1 + \sum_{i=1}^{P-1} c_i(\beta(\theta)^i + \beta(\theta)^{-i}) = 0$, and hence they cannot be detected. Similarly, a ULA without auxiliary sensor, which is the case studied in this paper, have similar problems. Consequently, when a signal impinges on the array from any of the blind angles, the DOA cannot be correctly estimated using (21) or (22). As shown in Section V, the spectrum of the proposed method will miss the signals coming from blind angles. For more discussion of the problem, see [19].

Moreover, it should be noted that the proposed method requires that $N \le M - 2P + 1$, which implies that the performance may degrade for some small size arrays, e.g., $M \le 6$, since generally $2 \le M \le 4$. In addition, the proposed method mainly focuses on ULAs. Methods for some other array geometries have also been studied [16, 21]. In [21] an algorithm to jointly estimate the DOAs and mutual coupling coefficients for UCAs has been proposed. The special structure of the MCM of a UCA is utilized to develop an algorithm for jointly estimating the DOA and mutual coupling coefficients. Its effectiveness was verified by computer simulation. Though both the proposed method and this algorithm make use of the whole array instead of the subarray used in [19] to estimate the DOAs, different properties of the MCM are exploited in the two methods due to the difference in array geometry, which leads to different ways of parameterizing the steering vectors involved and estimating the mutual coupling coefficients. For the more difficult case of highly coupled arrays, the MCM in (4) may be required and the proposed method can also be used as an efficient initial guess to the classical method in [11]. We now consider the case where the DOAs are time varying.

IV. DOA TRACKING IN THE PRESENCE OF MUTUAL COUPLING

In most conventional subspace-based calibration methods, the DOAs of all signals were assumed to be time invariant. Consequently, the subspace would also be invariant and obtained through EVD from the entire samples. When the DOAs vary with time, the performance of conventional algorithms will be deteriorated significantly. To deal with this problem, three subspace tracking methods are developed below for tracking time-varying DOA in the presence of mutual coupling.

A. Modified Projection Approximation Subspace Tracking

First, we propose two effective variants of the PAST algorithm, namely MPAST and MOPAST algorithms which are, respectively, based on the conventional PAST [30] and OPAST [33] algorithms. According to PAST, the signal subspace can be obtained by minimizing the following objective function

$$\begin{aligned} J(\mathbf{W}(t)) &= \sum_{i=1}^{t} \eta^{t-i} \|\mathbf{x}(i) - \mathbf{W}(t)\mathbf{W}^{\mathrm{H}}(t)\mathbf{x}(i)\|^2 \\ &= \mathrm{tr}(\Omega(t)) - 2\mathrm{tr}(\mathbf{W}^{\mathrm{H}}(t)\Omega(t)\mathbf{W}(t)) \\ &\quad + \mathrm{tr}(\mathbf{W}^{\mathrm{H}}(t)\Omega(t)\mathbf{W}(t)\mathbf{W}^{\mathrm{H}}(t)\mathbf{W}(t)) \end{aligned} \tag{35}$$

where

$$\Omega(t) = \sum_{i=1}^{t} \eta^{t-i}\mathbf{x}(i)\mathbf{x}^{\mathrm{H}}(i) = \eta\Omega(t-1) + \mathbf{x}(t)\mathbf{x}^{\mathrm{H}}(t)$$

and $0 < \eta \le 1$ is the forgetting factor. As analyzed in [30], the column span of $\mathbf{W}$ is equal to that of the signal subspace $\mathbf{U}_S$, i.e.,

$$\mathrm{span}\{\mathbf{W}\} = \mathrm{span}\{\mathbf{U}_S\}. \tag{36}$$

As can be seen from (35), $J(\mathbf{W}(t))$ is a fourth-order function of $\mathbf{W}(t)$, which is rather difficult and expensive to minimize directly. Fortunately, a projection approximation was introduced in [30] to simplify this problem to the familiar RLS algorithm

TABLE II
The MPAST Algorithm

Initialize $\mathbf{P}_{(0)}(0)$ and $\mathbf{W}_{(0)}(0)$
For $t = 1,2,\ldots$ *do*
  $\mathbf{y}_{(0)}(t) = \mathbf{W}_{(0)}^{\mathrm{H}}(t-1)\mathbf{x}(t)$
  $\mathbf{h}_{(0)}(t) = \mathbf{P}_{(0)}(t-1)\mathbf{y}_{(0)}(t)$
  For $k = 1,2,\ldots,K$ *do*
    $\mathbf{g}_{(k)}(t) = \mathbf{h}_{(k-1)}(t)/[\eta + \mathbf{y}_{(k-1)}^{\mathrm{H}}(t)\mathbf{h}_{(k-1)}(t)]$
    $\mathbf{P}_{(k)}(t) = \frac{1}{\eta}\mathrm{Tri}\{\mathbf{P}_{(k-1)}(t-1) - \mathbf{g}_{(k)}(t)\mathbf{h}_{(k-1)}^{\mathrm{H}}(t)\}$
    $\mathbf{e}_{(k)}(t) = \mathbf{x}(t) - \mathbf{W}_{(k-1)}(t-1)\mathbf{y}_{(k-1)}(t)$
    if $\|\mathbf{e}_{(k)}(t)\| > \|\mathbf{e}_{(k-1)}(t)\|$ *break*; *end*
    $\mathbf{W}_{(k)}(t) = \mathbf{W}_{(k-1)}(t-1) + \mathbf{e}_{(k)}(t)\mathbf{g}_{(k)}^{\mathrm{H}}(t)$
    $\mathbf{P}_{(k)}(t-1) = \mathbf{P}_{(k)}(t)$
    $\mathbf{W}_{(k)}(t-1) = \mathbf{W}_{(k)}(t)$
    $\mathbf{y}_{(k)}(t) = \mathbf{W}_{(k)}^{\mathrm{H}}(t-1)\mathbf{x}(t)$
    $\mathbf{h}_{(k)}(t) = \mathbf{P}_{(k)}(t-1)\mathbf{y}_{(k)}(t)$
  end k
  $\mathbf{P}_{(0)}(t) = \mathbf{P}_{(K)}(t)$
  $\mathbf{W}_{(0)}(t) = \mathbf{W}_{(K)}(t)$
end t

TABLE III
The MOPAST Algorithm

Initialize $\mathbf{P}_{(0)}(0)$ and $\mathbf{W}_{(0)}(0)$
For $t = 1,2,\ldots$ *do*
  $\mathbf{y}_{(0)}(t) = \mathbf{W}_{(0)}^{\mathrm{H}}(t-1)\mathbf{x}(t)$
  $\mathbf{h}_{(0)}(t) = \mathbf{P}_{(0)}(t-1)\mathbf{y}_{(0)}(t)$
  For $k = 1,2,\ldots,K$ *do*
    $\mathbf{g}_{(k)}(t) = \mathbf{h}_{(k-1)}(t)/[\eta + \mathbf{y}_{(k-1)}^{\mathrm{H}}(t)\mathbf{h}_{(k-1)}(t)]$
    $\mathbf{P}_{(k)}(t) = \frac{1}{\eta}\mathrm{Tri}\{\mathbf{P}_{(k-1)}(t-1) - \mathbf{g}_{(k)}(t)\mathbf{h}_{(k-1)}^{\mathrm{H}}(t)\}$
    $\mathbf{e}_{(k)}(t) = \mathbf{x}(t) - \mathbf{W}_{(k-1)}(t-1)\mathbf{y}_{(k-1)}(t)$
    if $\|\mathbf{e}_{(k)}(t)\| > \|\mathbf{e}_{(k-1)}(t)\|$ *break*; *end*
    $\tau_{(k)}(t) = \|\mathbf{g}_{(k)}(t)\|^{-2}((1 + \|\mathbf{e}_{(k)}(t)\|^2\|\mathbf{g}_{(k)}(t)\|^2)^{-2} - 1)$
    $\tilde{\mathbf{e}}_{(k)}(t) = \tau_{(k)}(t)\mathbf{W}_{(k-1)}(t-1)\mathbf{g}_{(k)}(t) + (1 + \tau_{(k)}(t)\|\mathbf{g}_{(k)}(t)\|^2)\mathbf{e}_{(k)}(t)$
    $\mathbf{W}_{(k)}(t) = \mathbf{W}_{(k-1)}(t-1) + \tilde{\mathbf{e}}_{(k)}(t)\mathbf{g}_{(k)}^{\mathrm{H}}(t)$
    $\mathbf{P}_{(k)}(t-1) = \mathbf{P}_{(k)}(t)$
    $\mathbf{W}_{(k)}(t-1) = \mathbf{W}_{(k)}(t)$
    $\mathbf{y}_{(k)}(t) = \mathbf{W}_{(k)}^{\mathrm{H}}(t-1)\mathbf{x}(t)$
    $\mathbf{h}_{(k)}(t) = \mathbf{P}_{(k)}(t-1)\mathbf{y}_{(k)}(t)$
  end k
  $\mathbf{P}_{(0)}(t) = \mathbf{P}_{(K)}(t)$
  $\mathbf{W}_{(0)}(t) = \mathbf{W}_{(K)}(t)$
end t

with considerably reduced arithmetic complexity. More precisely, (35) can be rewritten as

$$J(\mathbf{W}(t)) = \sum_{i=1}^{t} \eta^{t-i}\|\mathbf{x}(i) - \mathbf{W}(t)\mathbf{y}(i)\|^2 \tag{37}$$

where

$$\mathbf{y}(i) = \mathbf{W}^{\mathrm{H}}(t)\mathbf{x}(i). \tag{38}$$

For slowly varying signals, (38) can be approximated by

$$\mathbf{y}(i) \approx \mathbf{W}^{\mathrm{H}}(i-1)\mathbf{x}(i). \tag{39}$$

Let $J'(\mathbf{W}(t))$ denote the corresponding approximation $J(\mathbf{W}(t))$ with $\mathbf{y}(i)$ approximated by (39). Next, we can approximate the signal subspace by minimizing $J'(\mathbf{W}(t))$ with the RLS algorithm, since $J'(\mathbf{W}(t))$ is now linear in the variable $\mathbf{W}(t)$ to be estimated. This leads to the conventional PAST algorithm.

Since (39) is an approximation of $\mathbf{W}(t)$ by $\mathbf{W}(t-1)$, it can be further improved if a better estimate of $\mathbf{W}(t)$ is available. Such an estimate can be obtained from the current PAST output. Therefore, it makes sense to repeat the PAST iteration with $\mathbf{W}(t-1)$ replaced by the current PAST iteration, and so on. We find that the performance of the PAST algorithm can be further improved by this iterative scheme and thus call this new algorithm modified PAST (MPAST) algorithm. The RLS-based MPAST algorithm for signal subspace tracking is summarized in Table II, where the operator $\mathrm{Tri}\{\cdot\}$ indicates that only the upper (or lower) triangular part of the matrix argument is calculated and its Hermitian transposed version is copied to the lower (or upper) triangular part, K is the number of iterations, and the subscript (k) denotes the kth iteration. When $K = 1$, the proposed MPAST will reduce to the conventional PAST. At each time instant, the PAST algorithm requires $O(N^2) + 3MN$ operations. Hence, the complexity of the MPAST algorithm is $K[O(N^2) + 3MN]$ which is comparable to the PAST algorithm. As K increases, it is expected that the estimation accuracy will be improved in exchange for increased computational complexity. Fortunately, we found that a small K, say, $K = 2$, can achieve a satisfactory performance and complexity tradeoff, which is demonstrated by computer simulation results presented in Section V.

Since the proposed subspace-based method in Table I requires the estimated subspace to be orthonormal, an additional step of reorthonormalization of $\mathbf{W}(t)$ in Table II has to be performed. The arithmetic complexity is however increased to $K[O(N^2 + MN^2) + 3MN]$. In order to reduce the arithmetic complexity due to reorthonormalization, an orthonormal version of the MPAST algorithm, called MOPAST algorithm, is proposed in Table III. It is an extension of the OPAST algorithm in [33], which produces an orthonormal subspace directly. The corresponding complexity is $K[O(N^2) + 4MN]$, which is lower than that of the MPAST algorithm with reorthonormalization.

It is worth mentioning that the tracking error of the PAST and OPAST may be large at the initial stage due to a limited number of samples. In order

to avoid error propagation in the iterations of the MPAST and MOPAST algorithms, the number of iterations K is made adaptive by monitoring the norm of the tracking error $\mathbf{e}(t)$. Once the norm of $\mathbf{e}(t)$ at the kth iteration, i.e., $\|\mathbf{e}_{(k)}(t)\|$, is larger than that of the previous iteration, i.e., $\|\mathbf{e}_{(k)}(t)\| > \|\mathbf{e}_{(k-1)}(t)\|$, the iteration will be terminated, and $\mathbf{W}_{(k-1)}(t)$ will be used as the estimated subspace. Significant improvement in tracking accuracy, especially during initial tracking, was observed in our simulations.

B. Kalman Filter-Based Subspace Tracking with Variable Number of Measurements

Since the RLS-based MPAST and MOPAST assume that the subspace is slowly time varying, its performance will be degraded when the subspace changes considerably. To overcome this problem, we develop a Kalman filter-based subspace tracking method, named the KFVM algorithm, for DOA tracking. More precisely, the following two equations are introduced to construct a linear state-space model for subspace tracking

$$\mathbf{W}^{\mathrm{T}}(t) = \Lambda(t)\mathbf{W}^{\mathrm{T}}(t-1) + \Xi(t) \tag{40}$$

$$\mathbf{x}^{\mathrm{T}}(t) = \mathbf{H}(t)\mathbf{W}^{\mathrm{T}}(t) + \Psi(t) \tag{41}$$

where $\mathbf{W}(t)$ is the subspace to be tracked, $\mathbf{x}(t)$ is the observation, $\Lambda(t)$ is the state transition matrix and it is chosen as an identity matrix in this paper to impose smoothness in the state estimates, $\Xi(t)$ and $\Psi(t)$ are innovation matrix and residual error, respectively. Similar to the PAST method, the observation matrix $\mathbf{H}(t)$ can be approximated as $\mathbf{x}^{\mathrm{T}}(t)\hat{\mathbf{W}}^{*}(t-1)$, where the superscript $*$ denotes the complex conjugate operation. However, using similar ideas of MPAST, in our Kalman filter-based algorithm, a better estimate of $\mathbf{H}(t)$ can be given by

$$\mathbf{H}(t) = \mathbf{x}^{\mathrm{T}}(t)\hat{\mathbf{W}}^{*}(t/t-1). \tag{42}$$

We now proceed to derive the KFVM algorithm which can be employed for subspace tracking based on the above state-space model. For the sake of simplicity, we adopt the following state-space model for derivation

$$\mathbf{z}(t) = \Lambda(t)\mathbf{z}(t-1) + \mathbf{w}(t) \tag{43}$$

$$\mathbf{u}(t) = \mathbf{H}(t)\mathbf{z}(t) + \delta(t) \tag{44}$$

where $\mathbf{z}(t)$ and $\mathbf{u}(t)$ are the state vector and observation vector respectively. $\Lambda(t)$ and $\mathbf{H}(t)$ are the state transition matrix and observation matrix; $\mathbf{w}(t)$and $\delta(t)$ are zero mean Gaussian noise with covariance matrix $\mathbf{Q}_w(t)$ and $\mathbf{R}_\delta(t)$, respectively. We know that the optimal mean square error (MSE) estimator can be obtained by the standard Kalman filter recursions as follows

$$\begin{aligned}
\hat{\mathbf{z}}(t/t-1) &= \Lambda(t)\hat{\mathbf{z}}(t-1/t-1)\\
\mathbf{P}(t/t-1) &= \Lambda(t)\mathbf{P}(t-1/t-1)\Lambda^{\mathrm{T}}(t) + \mathbf{Q}_w(t)\\
\mathbf{e}(t) &= \mathbf{u}(t) - \mathbf{H}(t)\hat{\mathbf{z}}(t/t-1)\\
\mathbf{K}(t) &= \mathbf{P}(t/t-1)\mathbf{H}^{\mathrm{T}}(t)[\mathbf{H}(t)\mathbf{P}(t/t-1)\mathbf{H}^{\mathrm{T}}(t) + \mathbf{R}_\delta(t)]^{-1}\\
\hat{\mathbf{z}}(t/t) &= \hat{\mathbf{z}}(t/t-1) + \mathbf{K}(t)\mathbf{e}(t)\\
\mathbf{P}(t/t) &= [\mathbf{I} - \mathbf{K}(t)\mathbf{H}(t)]\mathbf{P}(t/t-1)
\end{aligned}$$

where $\mathbf{e}(t)$ denotes the prediction error of the observation vector, $\hat{\mathbf{z}}(t/\tau)$, $(\tau = t-1, t)$ represents the estimate of $\mathbf{z}(t)$ given the measurements up to time instant τ, i.e., $\{\mathbf{u}(i), i \le \tau\}$ and $\mathbf{P}(t/\tau)$ is the corresponding covariance matrix of $\hat{\mathbf{z}}(t/\tau)$.

The Kalman filter algorithm above can be regarded as a least squares (LS) regression problem [34]. It can also be seen in (44) that a single measurement is used to update the state vector. Though the bias error in using a single measurement will be low when the system is fast time varying, the estimation variance will rise correspondingly. Actually, when the system is time invariant or slowly time varying, more measurements in the past should be used to reduce the estimation variance, which leads to the proposed KFVM with better bias-variance tradeoff.

Suppose the measurements for tracking the state estimate at the time instant t are $\mathbf{u}(t-L(t)+1), \ldots, \mathbf{u}(t-1), \mathbf{u}(t)$, where $L(t)$ is the number of measurements used to update the state estimate. With this set of measurements, the linear state-space model of (40) and (41) can be extended as

$$\begin{bmatrix} \mathbf{I} \\ \mathbf{H}(t-L(t)+1) \\ \vdots \\ \mathbf{H}(t-1) \\ \mathbf{H}(t) \end{bmatrix} \mathbf{z}(t) = \begin{bmatrix} \Lambda(t)\hat{\mathbf{z}}(t-1/t-1) \\ \mathbf{u}(t-L(t)+1) \\ \vdots \\ \mathbf{u}(t-1) \\ \mathbf{u}(t) \end{bmatrix} + \Delta(t) \tag{45}$$

where

$$\Delta(t) = \begin{bmatrix} \Lambda(t)[\mathbf{z}(t-1) - \hat{\mathbf{z}}(t-1/t-1)] + \mathbf{w}(t) \\ -\delta(t-L(t)+1) \\ \vdots \\ -\delta(t) \end{bmatrix}$$

and

$$\begin{aligned}
&E[\Delta(t)\Delta^{\mathrm{T}}(t)]\\
&= \begin{bmatrix} \mathbf{P}(t/t-1) & 0 \\ \mathbf{0} & \mathrm{diag}\{\mathbf{R}_\delta(t-L(t)+1), \ldots, \mathbf{R}_\delta(t-1), \mathbf{R}_\delta(t)\} \end{bmatrix}\\
&= \mathbf{S}(t)\mathbf{S}^{\mathrm{T}}(t)
\end{aligned}$$

where $E[\cdot]$ denotes mathematical expectation and $\mathbf{S}(t)$ can be computed from the Cholesky decomposition of $E[\Delta(t)\Delta^{\mathrm{T}}(t)]$. Multiplying both sides of (45) by

$\mathbf{S}^{-1}(t)$will lead to a linear regression as follows

$$\mathbf{X}(t) = \bar{\mathbf{H}}(t)\mathbf{z}(t) + \xi(t) \tag{46}$$

where

$$\mathbf{X}(t) = \mathbf{S}^{-1}(t)\begin{bmatrix} \Lambda(t)\hat{\mathbf{z}}(t-1/t-1) \\ \mathbf{u}(t-L(t)+1) \\ \vdots \\ \mathbf{u}(t-1) \\ \mathbf{u}(t) \end{bmatrix}$$

$$\bar{\mathbf{H}}(t) = \mathbf{S}^{-1}(t)[\mathbf{I} \quad \mathbf{H}^{\mathrm{T}}(t-L(t)+1)\cdots\mathbf{H}^{\mathrm{T}}(t-1) \quad \mathbf{H}^{\mathrm{T}}(t)]^{\mathrm{T}}$$

$$\xi(t) = -\mathbf{S}^{-1}(t)\Delta(t).$$

It can be seen that (46) is a LS regression problem with solution

$$\hat{\mathbf{z}}(t) = (\bar{\mathbf{H}}^{\mathrm{T}}(t)\bar{\mathbf{H}}(t))^{-1}\bar{\mathbf{H}}^{\mathrm{T}}(t)\mathbf{X}(t) \tag{47}$$

and the covariance of estimating $\mathbf{z}(t)$ is

$$E[(\mathbf{z}(t)-\hat{\mathbf{z}}(t))(\mathbf{z}(t)-\hat{\mathbf{z}}(t))^{\mathrm{T}}] = \bar{\mathbf{P}}(t/t) = (\bar{\mathbf{H}}^{\mathrm{T}}(t)\bar{\mathbf{H}}(t))^{-1}. \tag{48}$$

As can be seen above, the number of measurements L is assumed to be time dependent. Particularly, if L is unchanged for all the time instants, a Kalman filter with multi-measurements (KFMM) results. Choosing L adaptively in KFVM has the advantage of achieving a better bias-variance tradeoff at each time instant. The scheme previously proposed in [35], [36] can be utilized here to select L at each time t. First, we define

$$\hat{\mathbf{e}}(t) = \hat{\mathbf{z}}(t-1) - \tilde{\mathbf{z}}(t-1) \tag{49}$$

$$\tilde{\mathbf{z}}(t) = \eta\tilde{\mathbf{z}}(t-1) + (1-\eta)\hat{\mathbf{z}}(t-1) \tag{50}$$

where $\hat{\mathbf{z}}(t)$ is the state estimate and $\hat{\mathbf{e}}(t)$ is its approximated time derivative. η is the forgetting factor $(0 < \eta \leq 1)$ for calculating the smoothed tap weight $\tilde{\mathbf{z}}(t)$. When the algorithm is about to converge to the signal subspace in a static environment, the l_1 or l_2 norms of $\hat{\mathbf{e}}(t)$ will decrease and converge gradually from its initial value to a very small value. Therefore, they serve as a measure of the variation of the signal subspace. To determine the number of measurements $L(t)$, the variable forgetting factor control scheme developed in [37] is utilized here. The absolute value of the approximate derivative of $\|\hat{\mathbf{e}}(t)\|$ is first computed as

$$G_e(t) = |\,\|\hat{\mathbf{e}}(t)\| - \|\hat{\mathbf{e}}(t-1)\|\,|. \tag{51}$$

Then it is smoothed to obtain $\bar{G}_e(t)$ by averaging it over a time window of length T_s. The initial value of $\bar{G}_e(t)$, denoted by $\bar{G}_{e0}$, is obtained by averaging the first T_s data. From simulation, we found that $T_s = 100$ gives satisfactory results. By normalizing $\bar{G}_e(t)$ with $\bar{G}_{e0}$, we get $\bar{G}_N(t)$, which is a more stable measure of the subspace variation. From this, we propose to update $L(t)$ at each snapshot as

$$L(t) = L_L + [1 - g(\bar{G}_N(t))](L_U - L_L) \tag{52}$$

where L_L and L_U are, respectively, the lower and upper bounds of $L(t)$ and

$$g(x) = \begin{cases} 1, & x \geq 1 \\ x, & 0 < x < 1 \\ 0, & x \leq 0 \end{cases}$$

is a clipping function which keeps the range of $\bar{G}_N(t)$ to the interval $[0,1]$. We can see that more measurements will be used if the subspace variation measure $\bar{G}_N(t)$ is small and vice versa.

To further stabilize the adaptive number of measurements, time-recursive forward smoothing similar to the conventional forgetting-factor-based method can be employed. More precisely $L(t)$ can be recursively estimated as

$$L(t) = \lambda_L L_L + (1-\lambda_L)\{L_L + [1 - g(\bar{G}_N(t))](L_U - L_L)\} \tag{53}$$

where $0 < \lambda_L \leq 1$ is a forgetting factor. Hence, the new KFVM algorithm can be obtained by using $L(t)$ number of measurements to estimate the system state.

Consequently, the above derived KFVM algorithm can be directly applied to the state-space model in (40) and (41) by adaptively employing $L(t)$ measurements, i.e., $\mathbf{x}(t-L(t)+1),\ldots,\mathbf{x}(t-1),\mathbf{x}(t)$, for updating the subspace $\mathbf{W}(t)$. It can be seen that different from conventional Kalman filter or RLS-based tracking algorithms, the main advantage of the proposed method is that the number of observations is adaptively chosen. In other words, when the system is fast time varying, a small number of measurements are chosen to reduce the bias error. When the system is slowly time varying, more measurements are used to reduce the estimation variance. Hence, the proposed KFVM can achieve a better bias-variance trade off. It should be noted that since $\mathbf{W}(t)$ is not exactly orthonormal, an additional reorthonormalization step is needed when orthonormality is required. The detailed procedure of this KFVM-based subspace tracking algorithm is summarized in Table IV.

The resultant KFVM algorithm requires $O(L^3 + MN^2) + (L+1)MN + 2LN^2 + L^2N$ operations in each update when L measurements and orthonormalization are used. If $L \gg M$ and $L \gg N$, the complexity of KFVM is around $O(L^3)$, which will be higher than the PAST-based algorithms. If L is small, the complexity is comparable to PAST-based algorithms.

C. Subspace-Based DOA Tracking

Once the orthonormal signal subspace is obtained from the MPAST, MOPAST, or KFVM-based subspace tracking algorithms presented above, the DOAs can be tracked as follows. Since the

TABLE IV
The KFVM Algorithm

Initialize $\mathbf{P}(0)$, $\mathbf{W}(0)$, and $L(0)$
For $t = 1,2,\ldots,T_s$, *do*
i) Calculate $\hat{\mathbf{e}}(t)$ as (49) and (50).
ii) Calculate $G_e(t)$ as (51).
iii) Estimate $\mathbf{W}(t)$ using the standard Kalman filter.
end t
At time $t = T_s$, obtain $\bar{G}_{e0}$ by averaging first T_s estimates $G_e(t)$.
For $t = T_s + 1, T_s + 2, \ldots$ *do*
i) Calculate $\hat{\mathbf{e}}(t)$ as (49) and (50).
ii) Calculate $G_e(t)$ as (51) and obtain $\bar{G}_N(t)$ by normalizing $\bar{G}_e(t)$ with $\bar{G}_{e0}$.
iii) Update $L(t)$ as (51)–(53).
iv) Estimate $\mathbf{W}(t)$ using the KFVM with $L(t)$ measurements as (45)–(47).
end t

orthonormalized signal subspace $\mathbf{U}_S(t)$ and the noise subspace $\mathbf{U}_V(t)$ satisfy

$$\mathbf{U}_S(t)\mathbf{U}_S^{\mathrm{H}}(t) + \mathbf{U}_V(t)\mathbf{U}_V^{\mathrm{H}}(t) = \mathbf{I} \tag{54}$$

then $\mathbf{U}_V(t)\mathbf{U}_V^{\mathrm{H}}(t)$ in (20) can be computed as

$$\mathbf{U}_V(t)\mathbf{U}_V^{\mathrm{H}}(t) = \mathbf{I} - \mathbf{U}_S(t)\mathbf{U}_S^{\mathrm{H}}(t). \tag{55}$$

The DOAs at each time instant t can then be estimated from the angles associated with the peaks of the determinant-based spectrum

$$P_{\mathrm{DET}}(\theta,t) = \{\det[\mathbf{Q}(\theta,t)]\}^{-1} \tag{56}$$

or the eigenvalue-based spectrum

$$P_{\mathrm{EV}}(\theta,t) = \lambda_{\min}^{-1}[\mathbf{Q}(\theta,t)] \tag{57}$$

where

$$\mathbf{Q}(\theta,t) = \mathbf{T}^{\mathrm{H}}(\theta)\mathbf{U}_V(t)\mathbf{U}_V^{\mathrm{H}}(t)\mathbf{T}(\theta). \tag{58}$$

V. SIMULATION RESULTS

A. DOA and Mutual Coupling Estimation in Stationary Environments

Consider a ULA with $M = 10$ sensors, each separated by half wavelength, i.e., $d = 0.5\lambda$. The mutual coupling is assumed to be negligible at a distance larger than 1.5λ and hence $P = 3$. The corresponding two mutual coupling coefficients are assumed to be $c_1 = 0.65\exp(-j\pi/7)$ and $c_2 = 0.25\exp(-j\pi/10)$. Two uncorrelated narrowband signals with equal power impinge on the array from the far-field with directions $\theta_1 = 10^\circ$ and $\theta_2 = 30^\circ$, and 500 snapshots are obtained. In this simulation, the DOAs and mutual coupling are assumed to be stationary, so that mutual coupling coefficients and signal DOAs are constant. First, the background observation noise is assumed to be an AWGN with an SNR of 10 dB. The spatial spectra of our proposed method (21) and that proposed by Ye and Liu [19] are illustrated in Fig. 1, where the MUSIC algorithm with known mutual coupling is also shown for comparison.

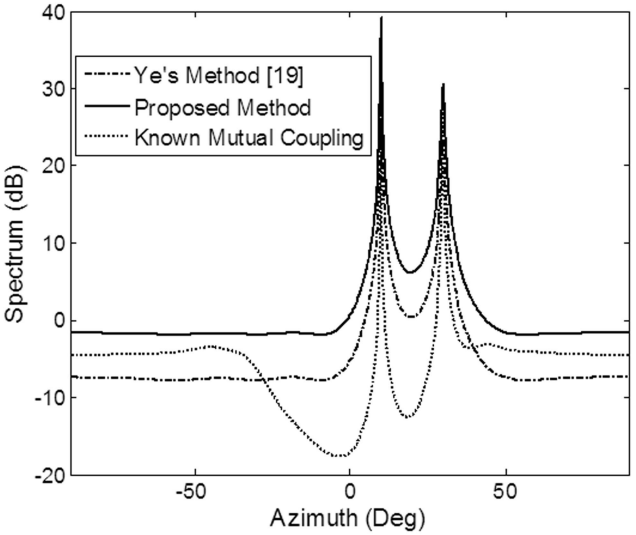

Fig. 1. Comparison of spectra of different methods (500 snapshots, SNR = 10 dB).

It can be seen that both of the methods work well at an SNR of 10 dB.

Next, the performance of the proposed method at different SNRs is evaluated. A hundred Monte-Carlo simulations are run at a set of different SNR levels from −5 dB to 20 dB and 500 snapshots are obtained for each experiment. The root mean squared error (RMSE) criterion is employed to assess and compare the DOA estimation results of different algorithms in a quantitative manner, and it is calculated as

$$\mathrm{RMSE} = \sqrt{\sum_{i=1}^{K_T}\sum_{n=1}^{N}(\theta_n - \hat{\theta}_{i,n})^2/(K_T N)}$$

where K_T is the number of Monte-Carlo experiments, N is the number of signals, θ_n is the nth DOA, and $\hat{\theta}_{i,n}$ denotes the nth estimated DOA in the ith Monte-Carlo experiment. The RMSE versus SNR curves are illustrated in Fig. 2. It is shown that the proposed method, which uses the whole array to estimate DOAs, outperforms the method in [19] at low SNR levels. The superiority of the proposed method gradually diminishes with the increase of SNR. When the SNR is larger than 5 dB, the proposed method has a comparable performance to the method in [19]. The estimated mutual coupling coefficients under different SNRs are listed in Tables V–VIII. The above results show that the proposed method can achieve satisfactory estimation accuracy, especially for small SNRs. One possible explanation is that comparing with the middle subarray, using the whole array has potential advantages such as a lower Cramér-Rao bound for DOA estimation as studied in [22]–[26]. Hence, the proposed method is able to give a better performance for DOA estimation and array calibration.

TABLE V
Estimated Amplitude of c_1 Against SNR (True Value $\rho_1 = 0.65$)

SNR	Ye's Method [19]		Proposed Method	
	$\hat{\rho}_1$	$\lvert\rho_1 - \hat{\rho}_1\rvert$	$\hat{\rho}_1$	$\lvert\rho_1 - \hat{\rho}_1\rvert$
−5 dB	0.5082	0.1418	0.6261	0.0239
−3 dB	0.5912	0.0588	0.6318	0.0182
−1 dB	0.6204	0.0296	0.6473	0.0027
1 dB	0.6241	0.0259	0.6407	0.0093
3 dB	0.6456	0.0044	0.6511	0.0011
5 dB	0.6481	0.0019	0.6473	0.0027

TABLE VI
Estimated Amplitude of c_2 Against SNR (True Value ρ_2=0.25)

SNR	Ye's Method [19]		Proposed Method	
	$\hat{\rho}_2$	$\lvert\rho_2 - \hat{\rho}_2\rvert$	$\hat{\rho}_2$	$\lvert\rho_2 - \hat{\rho}_2\rvert$
−5 dB	0.2805	0.0305	0.2573	0.0073
−3 dB	0.2671	0.0171	0.2586	0.0086
−1 dB	0.2600	0.0100	0.2523	0.0023
1 dB	0.2567	0.0067	0.2535	0.0035
3 dB	0.2518	0.0018	0.2521	0.0021
5 dB	0.2509	0.0009	0.2521	0.0021

TABLE VII
Estimated Phase of c_1 Against SNR
(True Value $\varphi_1 = -0.4488$ rad)

SNR	Ye's Method [19]		Proposed Method	
	$\hat{\phi}_1$	$\lvert\phi_1 - \hat{\phi}_1\rvert$	$\hat{\phi}_1$	$\lvert\phi_1 - \hat{\phi}_1\rvert$
−5 dB	−0.5127	0.0639	−0.4755	0.0267
−3 dB	−0.4620	0.0132	−0.4728	0.0240
−1 dB	−0.4588	0.0100	−0.4399	0.0089
1 dB	−0.4610	0.0122	−0.4733	0.0245
3 dB	−0.4468	0.0020	−0.4539	0.0051
5 dB	−0.4475	0.0013	−0.4480	0.0008

TABLE VIII
Estimated Phase of c_2 Against SNR
(True Value $\varphi_2 = -0.3142$ rad)

SNR	Ye's Method [19]		Proposed Method	
	$\hat{\phi}_2$	$\lvert\phi_2 - \hat{\phi}_2\rvert$	$\hat{\phi}_2$	$\lvert\phi_2 - \hat{\phi}_2\rvert$
−5 dB	−0.2516	0.0626	−0.2645	0.0497
−3 dB	−0.2803	0.0339	−0.2800	0.0342
−1 dB	−0.2951	0.0191	−0.3113	0.0029
1 dB	−0.3025	0.0017	−0.3109	0.0033
3 dB	−0.3069	0.0073	−0.3204	0.0062
5 dB	−0.3129	0.0013	−0.3124	0.0018

Thirdly, the iterative refinement in Step 8 of the proposed algorithm in Table I is applied to both of the methods. It is shown in Figs. 2 and 3 that the performances of both methods improve with the number of iterations. The proposed method converges considerably faster than the Ye's method, and its performance is close to that of known mutual coupling with only one additional iteration.

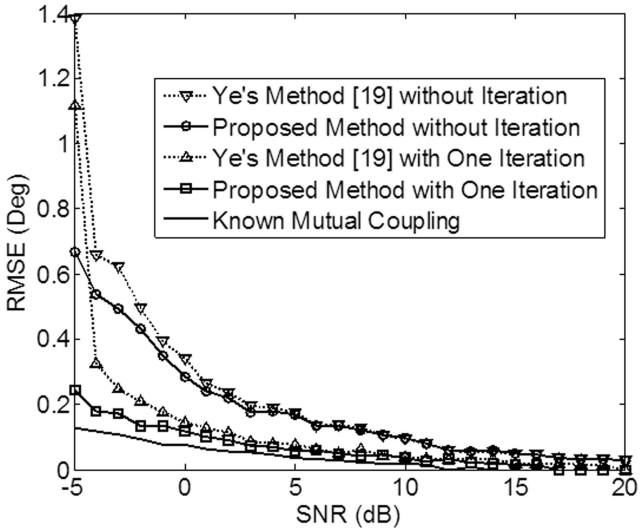

Fig. 2. Comparison of RMSEs of DOA using different methods (1 iteration) under different SNR values in stationary environment.

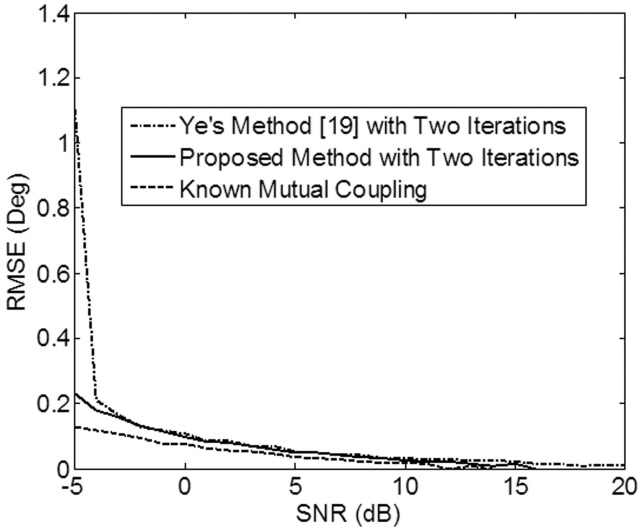

Fig. 3. Comparison of RMSEs of DOA using different methods (2 iterations) under different SNR values in stationary environment.

Finally, we illustrate the influence of blind angles on the proposed method. Following the settings of the first experiment in this section, we only change the mutual coupling coefficients to be $c_1 = 0.9081 + 0.0256j$ and $c_2 = -0.1880 - 0.0582j$, which have been utilized in the first simulation of [19]. Hence, there will be two blind angles, i.e., $-45°$ and $45°$. Fig. 4 shows the spectra of the proposed method (21), the method of [19], and the MUSIC algorithm with known mutual coupling. Comparing with the results in the first experiment, we notice that when there are no signals coming from the blind angles, the proposed method and the method of [19] performs quite well and there are no pseudopeaks of these two methods. However, the MUSIC algorithm with known mutual coupling coefficients has two pseudopeaks at the blind angles, and they generally do not affect

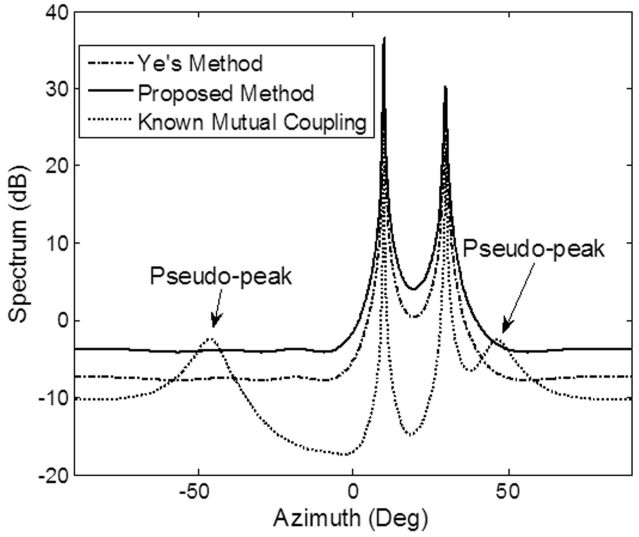

Fig. 4. Spectra of different methods under some special mutual coupling coefficients (500 snapshots, SNR = 10 dB).

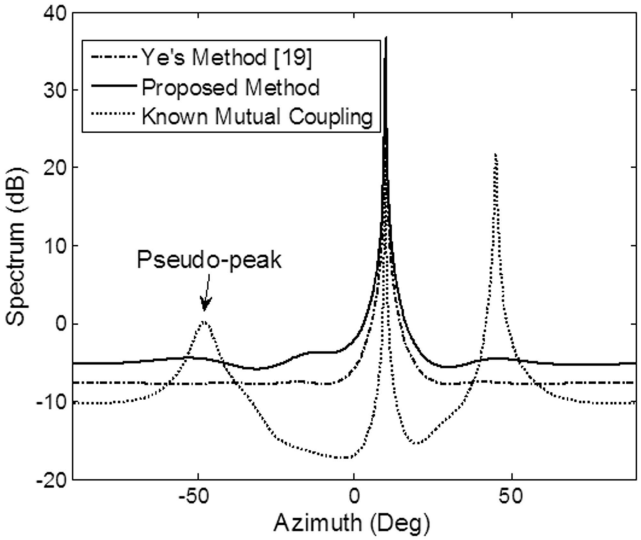

Fig. 5. Spectra of different methods when there exists a signal coming from blind angle 45° (500 snapshots, SNR = 10 dB).

much the DOA estimation since the peak values are comparatively small in the tested case. Next, based on the above settings, we change θ_2 to be 45°, i.e., the second signal comes from a blind angle. The resultant spectra are illustrated in Fig. 5. It can be seen from the spectra of the proposed method and the method of [19] that the second signal from 45° is missed, whereas the MUSIC algorithm with known mutual coupling can give satisfactory performance though there is a small pseudopeak at another blind angle.

B. DOA Tracking in Dynamic Environments

In this experiment, the tracking performances of the proposed MPAST and MOPAST algorithms in a dynamic DOA environment are tested. θ_1 is assumed to be invariant while θ_2 is assumed to be changing linearly and slowly according to the following model

$$\theta_2(t) = 30 - 1.5 \times 10^{-2} t, \qquad 0 \le t \le 800. \quad (59)$$

Here and in the following simulations, the unit for θ_1 and θ_2 is degree. The mutual coupling coefficients are assumed to be invariant and the SNR is 20 dB. The forgetting factors of the various PAST-based algorithms are set to $\eta = 0.98$, and hence the window length is approximately equal to 50. $\mathbf{P}_{(0)}(0)$ and $\mathbf{W}_{(0)}(0)$ of the proposed MPAST and MOPAST are initialized to identity matrices.

As a comparison, EVD [30], PAST, and OPAST algorithms are also implemented. However, the following simulation results and those in Section VC show that the performance of the OPAST algorithm is nearly identical to that of EVD and PAST algorithms after reorthonormalization, whereas the performance of the MOPAST algorithm is nearly identical to that of the MPAST algorithm after reorthonormalization. Therefore, we only focus on the results obtained using OPAST and MOPAST algorithms for clarity.

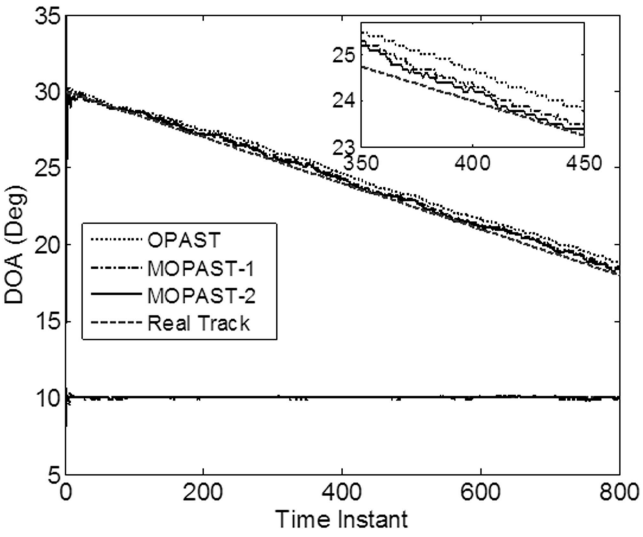

Fig. 6. Comparison of DOA tracking results using OPAST and MOPAST (MOPAST-1 and MOPAST-2 denote the MOPAST algorithm with one and two additional iterations, respectively) for time-varying DOA and invariant mutual coupling.

Fig. 6 shows the tracking results of different methods using a single experimental run. It can be seen that the MOPAST algorithm with one iteration (MOPAST-1) can achieve a better performance than the OPAST algorithm, and the performance of MOPAST for DOA tracking can be further improved with an increasing number of iterations, at the expense of higher computational complexity. Fortunately, simulation results show that MOPAST can generally achieve a satisfactory result with only one iteration.

We next compare the tracking performances of the OPAST, MOPAST, KFMM, and KFVM algorithms in a rapidly changing DOA environment. For illustration, θ_2 is assumed to undergo a sharp change in the time interval [600,620] according to the following

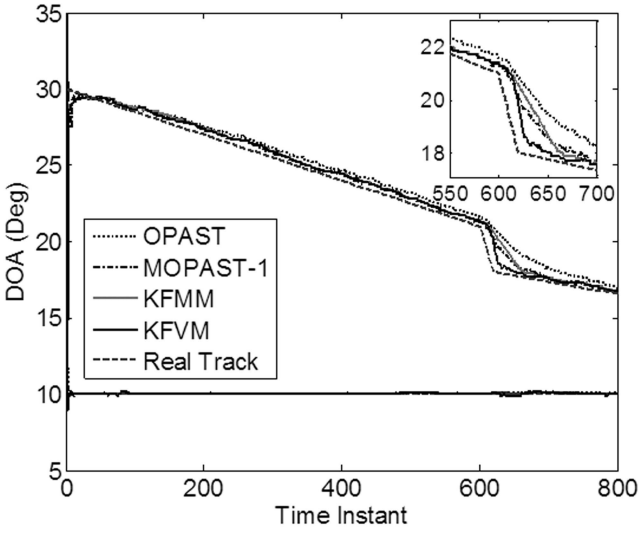

Fig. 7. Comparison of DOA tracking results using OPAST, MOPAST-1, KFMM ($L = 50$), and KFVM for time-varying DOA with sudden change and invariant mutual coupling.

model

$$\theta_2(t) = \begin{cases} 30 - 1.5 \times 10^{-2} t, & 0 \le t < 600 \\ 21 - 1.5 \times 10^{-1}(t - 600), & 600 \le t \le 620 \\ 18 - 7.9 \times 10^{-3}(t - 620), & 620 < t \le 800 \end{cases}. \tag{60}$$

In the KFMM and KFVM algorithms, the state transition matrix $\Lambda(t)$ is chosen as an identity matrix to impose smoothness in the state estimates. In the KFVM algorithm, $T_s = 100$, $L_L = 1$, $L_U = 50$, and $\lambda_L = 0.9$. $\mathbf{P}(0)$ and $\mathbf{W}(0)$ of the algorithm are initialized to identity matrices, and $L(0) = 1$. Fig. 7 depicts the results of OPAST, MOPAST-1, KFMM with $L = 50$ and KFVM using a single experimental run. It can be seen that the proposed adaptive Kalman filter-based subspace tracking algorithm achieves a good performance in both fast-varying and slow-varying DOA environments. When the subspace changes quickly, the KFVM method has a better tracking performance than the OPAST, MOPAST and KFMM algorithms.

VI. CONCLUSION

A class of subspace-based methods for DOA estimation and tracking in the case of ULAs with mutual coupling are presented. Using a new parameterization of the steering vector based on the banded symmetric Toeplitz MCM model and the subspace principle, the DOAs and mutual coupling coefficients can be estimated simultaneously using the data from the whole array. Simulation results show that the proposed method has better performance than the method recently proposed by Ye and Liu, especially at low SNR. The proposed algorithm is further extended to estimate time-varying DOAs in the presence of mutual coupling by means of subspace tracking. Three effective subspace tracking algorithms, called MPAST, MOPAST, and KFVM, with different arithmetic complexities and tracking abilities are presented. The MPAST and MOPAST algorithm have relatively lower arithmetic complexities and are suitable for slowly changing subspace. The KFVM algorithm is more suitable for rapidly changing subspace, at the expense of higher arithmetic complexity. Simulation results demonstrate that these three algorithms offer high flexibility and effectiveness for tracking both DOAs and mutual coupling coefficients in various conditions.

ACKNOWLEDGMENT

The authors would like to thank Dr. K. M. Tsui for valuable suggestions, which greatly improved the presentation of this paper.

REFERENCES

[1] Schmidt, R. O.
Multiple emitter location and signal parameter estimation.
IEEE Transactions on Antennas and Propagation, **34**, 3 (Mar. 1986), 276–280.

[2] Roy, R. and Kailath, T.
ESPRIT-estimation of signal parameters via rotational invariance techniques.
IEEE Transactions on Acoustics, Speech and Signal Processing, **37**, 7 (July 1989), 984–995.

[3] Amar, A. and Weiss, A. J.
Direct position determination of multiple radio signals.
In *Proceedings of the IEEE International Conference on Acoustics, Speech, and Signal Processing* (ICASSP), Montreal, Canada, May 2004, II-81–84.

[4] Astley, D., Swindlehurst, A. L., and Ottersten, B.
Spatial signature estimation for uniform linear arrays with unknown receiver gain and phases.
IEEE Transactions on Signal Processing, **47**, 8 (Aug. 1999), 2128–2138.

[5] Ho, K. C. and Yang, L.
On the use of a calibration emitter for source localization in the presence of sensor position uncertainty.
IEEE Transactions on Signal Processing, **56**, 12 (Dec. 2008), 5758–5772.

[6] Balanis, C.
Antenna Theory: Analysis and Design (2nd ed.).
Hoboken, NJ: Wiley, 1998.

[7] Dandekar, K. R., Ling, H., and Xu, G.
Experimental study of mutual coupling compensation in smart antenna applications.
IEEE Transactions on Wireless Communication, **1**, 3 (July 2002), 480–487.

[8] Adve, R. S. and Sarkar, T. K.
Compensation for the effects of mutual coupling on direct data domain algorithms.
IEEE Transactions on Antennas and Propagation, **48** (Jan. 2000), 86–94.

[9] Ng, B. C. and See, C. M. S.
Sensor-array calibration using a maximum-likelihood approach.
IEEE Transactions on Antennas and Propagation, **44**, 6 (June 1996), 827–835.

[10] See, C. M. S.
Sensor array calibration in the presence of mutual coupling and unknown sensor gains and phases.
Electronics Letters, **30**, 5 (Mar. 1994), 373–374.

[11] Friedlander, B. and Weiss, A. J.
Direction finding in the presence of mutual coupling.
IEEE Transactions on Antennas and Propagation, **39**, 3 (Mar. 1991), 273–284.

[12] Sellone, F. and Serra, A.
A novel online mutual coupling compensation algorithm for uniform and linear arrays.
IEEE Transactions on Signal Processing, **55**, 2 (Feb. 2007), 560–573.

[13] Ye, Z., et al.
DOA estimation for uniform linear array with mutual coupling.
IEEE Transactions on Aerospace and Electronic Systems, **45**, 1 (Jan. 2009), 280–288.

[14] Hung, E. K. L.
A critical study of a self-calibration direction-finding method for arrays.
IEEE Transactions on Signal Processing, **42**, 2 (Feb. 1994), 471–474.

[15] Wang, B., Wang, L., and Chen, H.
A robust DOA estimation algorithm for uniform linear array in the presence of mutual coupling.
In *Proceedings of the IEEE Antennas and Propagation Society International Symposium*, Columbus, OH, 2003, 924–927.

[16] Lin, M. and Yang, L.
Blind calibration and DOA estimation with uniform circular arrays in the presence of mutual coupling.
IEEE Antennas and Wireless Propagation Letters, **5**, 1 (Dec. 2006), 315–318.

[17] Wang, B., Wang, Y., and Chen, H.
Array calibration of angularly dependent gain and phase uncertainties with instrumental sensors.
In *Proceedings of the IEEE International Symposium on Phased Array Systems and Technology*, Boston, MA, 2003, 182–186.

[18] Wang, B., Wang, Y., and Gao, Y.
Mutual coupling calibration with instrumental sensors.
Electronics Letters, **40**, 7 (Apr. 2004), 406–408.

[19] Ye. Z. and Liu, C.
On the resiliency of MUSIC direction finding against antenna sensor coupling.
IEEE Transactions on Antennas and Propagation, **56**, 2 (Feb. 2008), 371–380.

[20] Liao, B., Zhang, Z. G., and Chan, S. C.
A subspace-based method for DOA estimation of uniform linear array in the presence of mutual coupling.
In *Proceedings of the IEEE International Symposium on Circuits and Systems*, Paris, 2010, 1879–1882.

[21] Qi, C., et al.
DOA estimation and self-calibration algorithm for uniform circular array.
Electronics Letters, **41**, 20 (Sept. 2005), 1092–1094.

[22] Weiss, A. J., Willsky, A. S., and Levy, B. C.
Eigenstructure approach for array processing with unknown intensity coefficients.
IEEE Transactions on Acoustics, Speech and Signal Processing, **36**, 10 (Oct. 1988), 1613–1617.

[23] Pesavento, M., Gershman, A. B., and Wong, K. M.
Direction of arrival estimation in partly calibrated time-varying sensor arrays.
In *Proceedings of the International Conference on Acoustics, Speech and Signal Processing* (ICASSP), Salt Lake City, UT, May 2001, 3005–3008.

[24] Pesavento, M., Gershman, A. B., and Wong, K. M.
Direction finding in partly-calibrated sensor arrays composed of multiple subarrays.
IEEE Transactions on Signal Processing, **50**, 9 (Sept. 2002), 2103–2115.

[25] See, C. M. S. and Gershman, A. B.
Direction-of-arrival estimation in partly calibrated subarray-based sensor arrays.
IEEE Transactions on Signal Processing, **52**, 2 (Feb. 2004), 329–338.

[26] Wang, B., et al.
Array calibration of angularly dependent gain and phase uncertainties with carry-on instrumental sensors.
Science in China, Series F, Information Sciences, **47**, 6 (2004), 777–792.

[27] Sword, C. K., Simaan, M., and Kamen, E. W.
Multiple target angle tracking using sensor array outputs.
IEEE Transactions on Aerospace and Electronic Systems, **26** (Mar. 1990), 367–373.

[28] Sastry, C. R., Kamen, E. W., and Simaan, M.
An efficient algorithm for tracking the angles of arrival of moving targets.
IEEE Transactions on Aerospace and Electronic Systems, **39** (Jan. 1991), 242–246.

[29] Lo, K. W. and Li, C. K.
An improved multiple target angle tracking algorithm.
IEEE Transactions on Aerospace and Electronic Systems, **28** (July 1992), 797–805.

[30] Yang, B.
Projection approximation subspace tracking.
IEEE Transactions on Signal Processing, **43**, 1 (Jan. 1995), 95–107.

[31] Yang, B.
An extension of the PASTd algorithm to both rank and subspace tracking.
IEEE Signal Processing Letters, **2**, 9 (Sept. 1995), 179–182.

[32] Sanchez-Araujo, J. and Marcos, S.
An efficient PASTd-algorithm implementation for multiple direction of arrival tracking.
IEEE Transactions on Signal Processing, **47**, 8 (Aug. 1999), 2321–2324.

[33] Abed-Meraim, K., Chkeif, A., and Hua, Y.
Fast orthonormal PAST algorithm.
IEEE Signal Processing Letters, **7**, 3 (Mar. 2000), 60–62.

[34] Durovic, Z. M. and Kovacevic, B. D.
Robust estimation with unknown noise statistics.
IEEE Transactions on Automatic Control, **44**, 6 (June 1999), 1292–1296.

[35] Chan, S. C., Zhang, Z. G., and Zhou, Y.
A new adaptive Kalman filter-based subspace tracking algorithm and its application to DOA estimation.
In *Proceedings of the IEEE International Symposium on Circuits and Systems*, Island of Kos, Greece, 2006, 129–132.

[36] Zhang, Z. G., et al.
A novel method for nonstationary power spectral density estimation of cardiovascular pressure signals based on a Kalman filter with variable number of measurements.
Medical & Biological Engineering & Computing, **46**, 8 (May 2008), 789–797.

[37] Chen, H. H., et al.
Adaptive beamforming and recursive DOA estimation using frequency-invariant uniform concentric spherical arrays.
IEEE Transactions on Circuits and Systems I, **55**, 10 (Nov. 2008), 3077–3089.

Bin Liao (S'09) received the B.Eng. and M.Eng. degrees from Xidian University, Xi'an, China, in 2006 and 2009, respectively.

He is currently pursuing the degree of Ph.D at the Department of Electrical and Electronic Engineering, the University of Hong Kong. His main research interests are array signal processing and adaptive filtering.

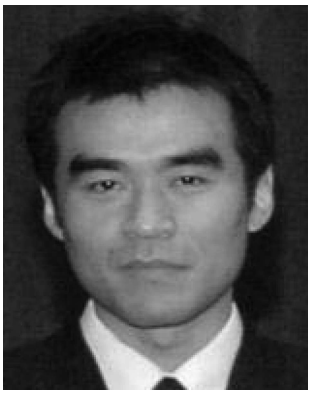

Zhi-Guo Zhang (M'07) received the B.Sc. and M.Eng. degrees in electrical and electronic engineering from Tianjin University and the University of Science and Technology of China in 2000 and 2003, respectively. He obtained the Ph.D. degree in 2008 from the Department of Electrical and Electronic Engineering at the University of Hong Kong, where he is currently a postdoctoral fellow.

His research interests are in the general areas of statistical signal processing and digital signal processing, and in particular, adaptive filtering, nonparametric regression, time frequency analysis, and biomedical signal processing.

Shing-Chow Chan (M'92) received the B.S. (Eng.) and Ph.D. degrees from the University of Hong Kong, Pokfulam, Hong Kong, in 1986 and 1992, respectively.

Since 1994, he has been with the University of Hong Kong and currently is an associate professor. He was a visiting researcher with Microsoft Corporation, Redmond, WA and Microsoft, Beijing, China, in 1998 and 1999, respectively. His research interests include fast transform algorithms, filter design and realization, multirate signal processing, and imagebased rendering.

Dr. Chan is currently an Associate Editor of the *IEEE Transactions on Circuits and Systems—I: Regular Papers* and the *Journal of Very Large Scale Integration Signal Processing and Video Technology*, and a member of the Digital Signal Processing Technical Committee of the IEEE Circuits and Systems Society. He has been the Chairman of the IEEE Hong Kong Chapter of Signal Processing from 2000 to 2002.